Nanostructures

DOI: 10.1002/ange.200906783

Asymmetric Dumbbells from Selective Deposition of Metals on Seeded Semiconductor Nanorods**

*Sabyasachi Chakrabortty, Jie An Yang, Yee Min Tan, Nimai Mishra, and Yinthai Chan**

A key goal in nanocrystal research has been the integration of different materials within the same nanostructure so that multiple functionalities may be incorporated. Promising examples of such structures are hybrid metal–semiconductor nanocomposites, in which a metal and its semiconductor nanoparticle counterpart are closely coupled so that novel properties or applications may emerge. For example, metal tips on semiconductor nanorods can serve as anchor points for electrical connections or for end-to-end self-assembly into complex structures,[1] while improved charge separation at the metal–semiconductor interface can enhance photocatalytic processes.[2] Addition of the metal to a semiconductor nanoparticle can also modify its nonlinear optical response[3] or impart magnetic functionality.[4] Recently, there has been some interest in utilizing seeded semiconductor nanorods as building blocks for generating hybrid metal–semiconductor nano-heterostructures, since their optical and chemical properties can be adjusted by both the core and its anisotropic shell.[5] Growth of Pt,[6] Au,[1d,7] and Co[4c] on such nanorods have been reported.

Previous efforts to grow Au nanoparticles on CdSe-seeded CdS nanorods showed that deposition of Au can occur at the tips of the rod or at the location of the CdSe seed by an electrochemical Ostwald ripening process.[7a] Under UV excitation, large Au domains may be exclusively deposited at one end of the seeded CdSe/CdS rod because of electron migration to one of the metal tips,[7b,8a] whereas under ambient light conditions, the deposition of Au along the nanorod is strongly influenced by temperature-dependent, ligand-mediated defect sites.[8a] Precise control over the deposition of Au at specific locations on the anisotropic core–shell rod would not only be critical for directed assembly, but should also have a dramatic influence on the optical properties of the rod. Achieving this goal by a facile, straightforward method that obviates the need for stringent control over multiple parameters would thus be highly desirable. Herein, we demonstrate that good control over the deposition of Au on seeded CdSe/CdS nano-heterostructures may be obtained under ambient light conditions by simply varying the concentration of the added Au precursor, and results in well-defined, Au-decorated surface morphologies. By only varying the precursor concentration, we further show that control over the morphology of the less-studied Ag_2S–CdSe/CdS hybrid nanorod heterostructures can be achieved, where systematic exposure of seeded CdSe/CdS nanorods to different concentrations of Ag^+ ions afforded morphological changes similar to those of the Au–CdSe/CdS system, despite differences in their mechanisms of formation. We subsequently show that the sequential deposition of Au and Ag precursors to the seeded CdSe/CdS nanorods can result in novel and structurally defined "Janus-type" dumbbell structures, in which the material composition at one end of the dumbbell is different from that at the other end.

The difference in reactivities between the facets at the tips and at the sides of the CdS shell in the CdSe/CdS nano-heterostructure has been well-documented,[4c,5,8] and the likelihood of heterogeneous nucleation and growth of Au clusters at dissimilar sites on the nanorod is expected to be significantly different. For example, it was suggested that the anisotropic reactivity of the {001} and {00$\bar{1}$} tips of seeded CdSe/CdS nanorods resulted in attachment of Co nanoparticles to only one side of the rod.[4c] The resulting hierarchical order of free energy barriers to nucleation at different sites of the nanorod would then imply that preferential nucleation at the most reactive sites may be controlled by monomer concentration, as observed previously in Au–PbS nanocrystals.[9] To qualify this assertion, we firstly synthesized CdSe cores of about 2.5 nm in diameter by following a previously reported procedure,[10] which we modified slightly. Subsequent growth of the asymmetric CdS shell with various aspect ratios and shapes around the CdSe core was achieved by following the seeded growth approach of Manna and co-workers.[11] The resulting CdSe/CdS nano-heterostructures were then separated from the growth solution and dispersed in a mixture of toluene and ODPA (*n*-octadecylphosphonic acid). Gold growth proceeded after injection of the rod solution into a mixture of $AuCl_3$, tetraoctylammonium bromide (TOAB), and dodecylamine (DDA) in toluene. All reactions were carried out in an inert atmosphere at room temperature under ambient light conditions for a fixed amount of time (see the Supporting Information for details), with the concentration of the added Au precursors as the only variable.

[*] S. Chakrabortty, J. A. Yang, Y. M. Tan, N. Mishra, Prof. Y. Chan
Department of Chemistry, National University of Singapore
3 Science Drive 3, Singapore 117543 (Singapore)
E-mail: chmchany@nus.edu.sg
Prof. Y. Chan
Institute for Materials Research & Engineering
A*STAR, 3 Research Link
Singapore 117602 (Singapore)
Fax: (+65) 6779-1691
E-mail: chanyt@imre.a-star.edu.sg

[**] We thank M. Lin for EFTEM measurements. This work was supported by the National University of Singapore (start-up grant WBS R143-000-367-133) and the Institute of Materials Research & Engineering (project code IMRE/00-1C0288).

Supporting information for this article is available on the WWW under http://dx.doi.org/10.1002/anie.200906783.

Figure 1 a–c shows representative TEM images of the resultant CdSe-seeded CdS nano-heterostructures with Au deposited at distinct locations on their surface. The trend of

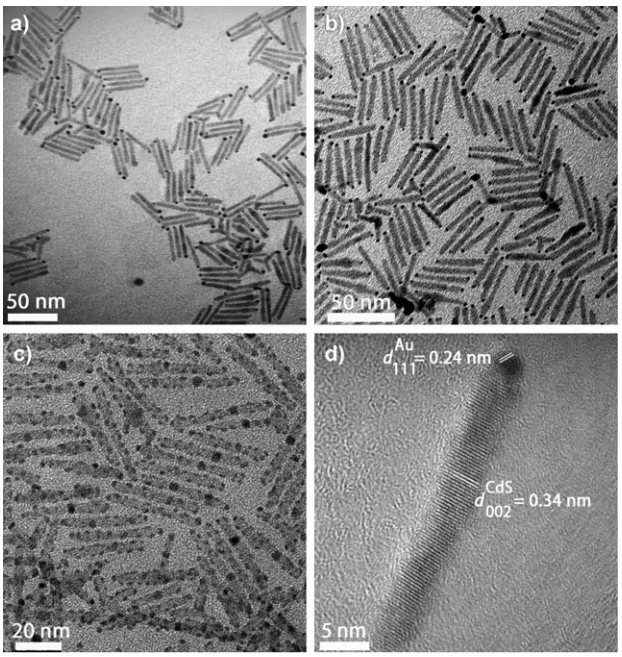

Figure 1. TEM images of CdSe-seeded CdS nano-heterostructures with controlled, varying degrees of Au deposition: CdSe/CdS nanorods with ca. 40 nm length and an aspect ratio of ca. 8 exposed to increasing concentrations of Au precursor, resulting in Au deposited at a) one end, b) both ends, and c) throughout the rod respectively; d) HRTEM image showing a gold nanoparticle at the apex of the nanorod. The measured *d*-spacing values from the visible lattice fringes 0.24 nm and 0.34 nm are assigned to Au (111) and CdS (002) respectively.

selective Au growth at one tip, two tips, and throughout the nanorod with increasing concentrations of added Au precursor was reproduced at a variety of fixed temperatures (25 °C–90 °C) and sufficiently long growth times (up to 6 h). This result is consistent with our hypothesis that a hierarchical order of reactivities exists between the facets at the tips and sides of the nanorod. Within the range of reaction times and temperatures explored, we found no evidence that the rods with Au at one tip were the result of Ostwald ripening, which was previously reported for Au–CdSe nanorods.[1a] Consistent with previous reports,[8a,12] high-resolution transmission electron microscopy (HRTEM) of the nanorod with Au at one tip (Figure 1 d) showed non-epitaxial growth at the apex of the CdS shell. Interestingly, selective growth of Au at the location of the CdSe core[7a] was rarely observed and was always accompanied by growth of particles throughout the rod at high concentrations of Au precursors. This growth may be due to use of ODPA in the gold deposition process, as ODPA has been shown to bind selectively to the {100} facets of CdS,[5] possibly reducing surface defects and sterically hindering the deposition of Au at the sides of the nanorod. While stabilizers such as (di-*n*-dodecyl)dimethylammonium bromide (DDAB) have previously been suggested to act as a slow etchant of CdS,[8a] we believe that given the mild reaction conditions, the use of the more sterically hindered TOAB does not play a significant role in directing the Au deposition process.

The hierarchy of reactivities with respect to Au deposition may be understood from the fact that the facets at the ends of the nanorod have a higher surface energy than the facets at the sides.[4c,5,8] Additionally, the facets at the fast-growing end, which is further from the CdSe core, tend to be sulfur-rich, while the facets at the end closer to the CdSe core tend to be cadmium-rich.[8a] The strong Au–S interaction indicates that Au deposition first occurs primarily on the facets at the end further from the CdSe core, followed by deposition on the facets at the end closer to the CdSe core. In order to elucidate the position of the Au tip relative to the CdSe core for the one-tipped rods, we employed S mapping by energy-filtered transmission electron microscopy (EFTEM), as previously established by Deka et al.[4c] As shown in Figure 2 a, b, the CdSe cores that could be identified typically showed that the Au tip was located at the end further from the CdSe core, though the S $L_{2,3}$ signal was generally weak[4c] because of the small size of the cores, and their positions on many of the rods could not be determined. We subsequently employed large 3.6 nm CdSe seeds and longer growth times during the nanorod synthesis, which yielded lance-shaped nanorods of about 70 nm in length. The bulge in the rods, which corresponded to the location of the CdSe core, afforded direct identification of its position in the nanorod (see the Supporting Information). Exposure to a sufficiently low concentration of the Au precursor resulted in deposition mostly at the end of the rod furthest from the CdSe core (Figure 2 c).

In rare instances where branching occurred from the bulge where the core resided, Au was also found to nucleate and grow at the tips of the branched arms, which likely have S-rich facets at their tips.[13] Taken together, the trends shown in Figure 1, the EFTEM data on the nanorods (ca. 40 nm × 5 nm), and the TEM data on the lance-shaped nanorods (ca. 70 nm × 6 nm) corroborate our hypothesis on hierarchical reactivities in which the Au deposits first at the apex furthest from the CdSe core, then at the apex closest to the CdSe core, and then finally at the facets located at the sides of the nanorod.

Exposure of the seeded CdSe/CdS nanorods to different concentrations of Ag^+ ions resulted in morphological changes similar to that of the Au–CdSe/CdS nanorods, despite the fact that Ag^+ ions undergo spontaneous cationic exchange with Cd^{2+} ions, as previously observed in CdS nanorods.[14] Investigation of this exchange process in the context of CdSe-seeded CdS nanorods proceeded as follows: briefly, uniform CdSe-seeded CdS nanorods were exposed to a solution containing toluene, ethanol, DDA, and $AgNO_3$ under ambient light at room temperature for a fixed amount of time. As in the case of Au, the concentration of the added Ag precursors was the only parameter varied. Figure 3 a, b show TEM images of seeded CdSe/CdS nanorods that were exposed to relatively low and high concentrations of Ag^+ ions, respectively. Analysis by HRTEM revealed CdSe/CdS nanorods coated with nanoparticles about 2.5 nm in diameter with visible lattice fringes that correspond to the {$\bar{1}$21} plane of Ag_2S and are consistent with a cationic exchange process

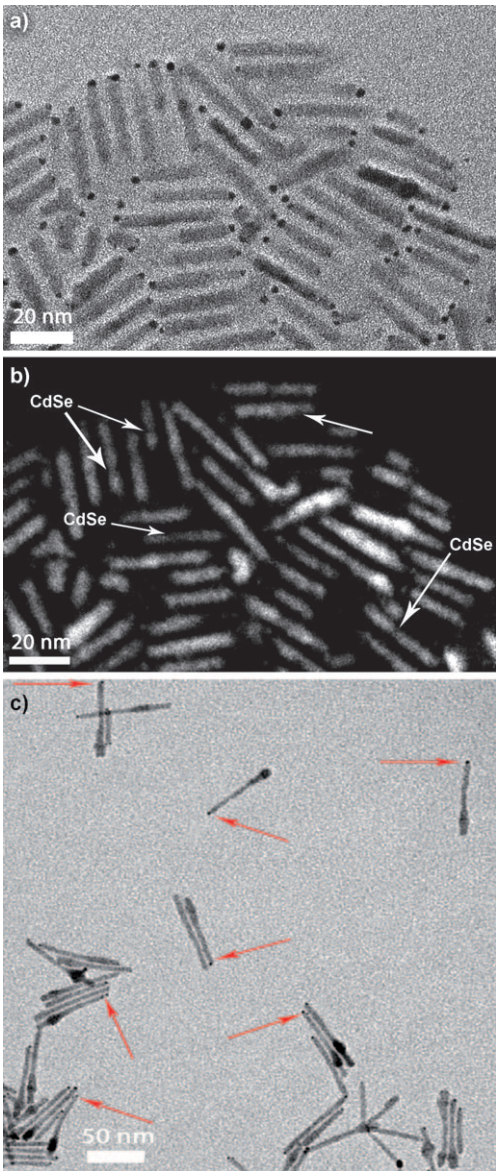

Figure 2. a) Elastic zero-loss EFTEM image of Au-tipped seeded CdSe/CdS nanorods. b) Corresponding inelastic EFTEM image with energy filtering at the S $L_{2,3}$ edge. The arrows (white) indicate areas of S absence, which can be ascribed to the presence of the CdSe cores. c) Lance-shaped nanorods (approximate dimensions: 70 nm length, 6 nm diameter, 10 nm diameter at the bulge) with Au at the end of the rod furthest from the CdSe core, whose approximate location is at the bulge of the rod. Arrows (red) indicate the location of the Au tip.

between Cd^{2+} and Ag^+. At high concentrations of Ag^+, nanoparticles of Ag_2S distributed at evenly spaced positions across the nanorod were seen, in accordance with previous findings on CdS nanorods.[14] A significant number of rods were also found to have Ag_2S located specifically above the location of the CdSe seed, as expected from the occurrence of more surface defects there.[7a,8a] Unlike in the case of the CdS nanorods,[14] however, exclusive formation of Ag_2S at the tips of the nanorods was obtained at low concentrations of Ag^+ ions. This observation suggests that the enhanced topological selectivity of seeded CdSe/CdS over CdS rods, which is

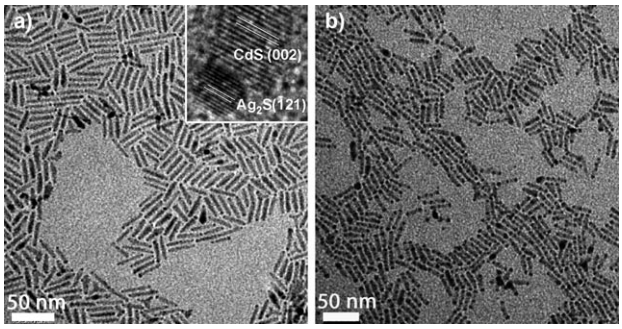

Figure 3. TEM images illustrating the morphology evolution of seeded CdSe/CdS nanorods with the concentration of Ag^+ ions as the only variable parameter. Exposure to low (a) and high (b) concentrations of Ag^+ ions resulted in the formation of Ag_2S nanoparticles exclusively at the tips and throughout the nanorod respectively. The inset in (a) is a HRTEM image showing the visible lattice fringes of the Ag_2S $\{\bar{1}21\}$ and CdS {002} planes with measured *d* spacings of 0.26 nm and 0.34 nm, respectively. Scale bar (inset): 5 nm.

typically discussed in the context of heterogeneous nucleation and growth, may also be applicable to the cationic exchange process. The relative distribution of one-tipped and two-tipped Ag_2S–CdSe/CdS nanorods in a given ensemble as a function of the concentration of added Ag^+ ions followed the same evolutionary trends as the Au–CdSe/CdS system. The distribution is commensurate with the notion that the facets at the ends of the asymmetric core–shell nanorod have anisotropic reactivity. However, the distinction between relative populations of rods with Ag_2S at one end and two ends was not as pronounced as in the case with Au, where selective deposition at one end versus two ends can be precisely controlled. A possible explanation may be the fact that the interaction of Ag with S is not as strong as that of Au with S (bond enthalpies are 217 kJ mol^{-1} and 418 kJ mol^{-1} for Ag–S and Au–S respectively),[15] and thus the affinity of the Ag precursors for the S-rich and Cd-rich facets on either ends of the nanorod is probably not as large as in the case of Au.

The optical characterization of the Ag_2S–CdSe/CdS nanorods by UV/Vis absorption and fluorescence measurements is summarized in Figure 4. A progressive decline in the number of discernible features of CdS in the absorption spectra with increasing amounts of Ag_2S nanoparticles (clearly shown in Figure 4a) may be attributed to: 1) the extent of Cd^{2+} ion

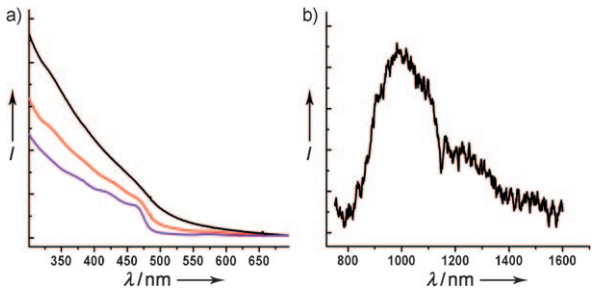

Figure 4. a) Absorption spectra of starting seeded CdSe/CdS nanorods (violet), rods shown in Figure 3a (red) and rods shown in Figure 3b (black). b) Photoluminescence spectra of rods shown in Figure 3b.

exchange varys from rod to rod, thus resulting in wider size/shape distributions that cover features in the size-dependent absorption spectra; and 2) coupling of Ag_2S and CdS electronic states. The emergence of increased absorbance at lower energies is expected from the fact that Ag_2S is a narrow-gap semiconductor with a bulk band gap of approximately 1 eV. It should be noted that comparison with mixtures of free Ag_2S nanoparticles and unperturbed CdSe/CdS nanorods to corroborate point 2 above, as investigated previously in metal–nanorod systems,[4b,c] is not a fair one in this case, since degradation of the CdS shell occurs through cationic exchange with Ag^+ ions. However, previous studies of Ag_2S–CdS nanorod systems have suggested coupling between Ag_2S and CdS at the heterojunction to form a Type I interface in which the fluorescence of CdS is quenched and NIR fluorescence from Ag_2S is observed.[14] In our case, the fluorescence from the excitonic recombination in the CdSe core from rods shown in Figure 3a is largely quenched, whilst the fluorescence from the rods in Figure 3b is totally quenched. Discernible NIR fluorescence with a peak emission of approximately 1000 nm[14] is seen from rods shown in Figure 3b (illustrated in Figure 4b), while much weaker NIR fluorescence is obtained for rods shown in Figure 3a (not shown). It is thus possible that a certain degree of coupling between the different materials does occur, though the exact mechanism for the observed quenching requires further investigation.

Given the high degree of control over the deposition process for Au and Ag_2S at the tips of CdSe-seeded CdS nanorods by varying the amount of added precursor, we investigated the possibility of fabricating "Janus-type" nanorod dumbbell structures where each end of the nanorod contains a nanoparticle with a different material composition. We hypothesized that the deposition of Au to obtain rods with Au only at one end would make the facets at that end inaccessible to Ag^+ ions. Thus the nanorods were first exposed Au and then the seeded CdSe/CdS nanorods with Au at one end were exposed to Ag precursors at concentrations that were sufficiently low to minimize cationic exchange at the sides of the rod, or nucleation and growth of free Ag nanoparticles in solution. Figure 5a shows a TEM image of nanorods after exposure to Ag^+, which resulted in most rods bearing nanoparticles at both ends. Nanorods with nanoparticles attached to their sides were rarely observed, which is indicative of the exquisite control over the deposition process. The presence of both Au and Ag was confirmed by energy-dispersive X-ray spectroscopy (EDX; see the Supporting Information), thus suggesting that the second deposition process did not cause the Au nanoparticles to detach from the nanorod. Analysis by HRTEM to ascertain the identities of the nanoparticles at each end of the rod revealed that most of the rods had Au at one end and Ag_2S at the other end, as shown in Figure 5b. Interestingly, *d* spacings from the visible lattice fringes on the Au nanoparticle occasionally showed the presence of Ag as well (see Supporting Information). This feature may be understood from the presence of DDA that was used during the exposure to Ag^+ ions. It is known that DDA can act as a mild reducing agent and a capping group for the nanorods,[1a,b] and it is thus possible that

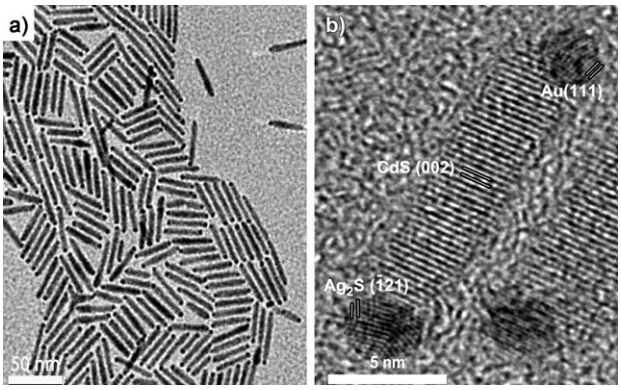

Figure 5. a) TEM image of seeded CdSe/CdS nanorods with Au nanoparticles at one end and Ag_2S nanoparticles at the other end. b) HRTEM image showing the visible lattice fringes of the Ag_2S {$\bar{1}$21} and Au {111} planes with measured *d* spacings of 0.26 nm and 0.24 nm, respectively.

Ag^+ ions that are in the vicinity of the Au nanoparticle can be reduced by DDA and can be deposited onto the Au surface. These preliminary findings suggest that the presence of a nanoparticle at the tip does to some extent prevent access to the reactive facets at that tip, thus allowing the other tip of the rod to support growth of another material. After long reaction times but sufficiently low Ag^+ ion concentrations, the deposition of Ag on the Ag_2S end could also seen (see the Supporting Information); this deposition was verified to also occur in our Ag_2S–CdSe/CdS system. Nevertheless, a judicious choice of Ag^+ ion concentrations and reaction times (unfortunately not strictly single-parameter in this case) should minimize the subsequent deposition of Ag on Ag_2S or Au.

In summary, we have demonstrated facile, single-parameter control over the deposition of Au nanoparticles at distinct locations on CdSe-seeded CdS nanorod heterostructures. A hierarchical order of reactivities between the different facets at the tips and sides of the nanorod was suggested as the underlying reason as to why different concentrations of Au precursors led to specific Au-decorated morphologies. The concentration of added Ag precursors as the only parameter varied was also found to produce similar morphological trends as the Au-CdSe/CdS nanorods, leading to CdSe/CdS nanorods with Ag_2S nanoparticles located exclusively at the tips of the rods. The relatively straightforward adjustment of precursor concentrations offered convenient and precise control over the deposition process, and allowed us to engineer novel "Janus-type" dumbbell structures with different nanoparticles at each tip. Further development on such "Janus-type" dumbbell structures with complex architectures would likely yield expanded chemical functionality and physical properties not achievable with symmetric nanorod dumbbells alone,[1a] thus opening up new avenues for applications.

Received: December 2, 2009
Published online: March 19, 2010

Keywords: gold · nanoparticles · nanostructures · semiconductors · silver

[1] a) T. Mokari, C. G. Sztrum, A. Salant, E. Rabani, U. Banin, *Nat. Mater.* **2005**, *4*, 855 – 863; b) T. Mokari, E. Rothenberg, I. Popov, R. Costi, U. Banin, *Science* **2004**, *304*, 1787 – 1790; c) A. Salant, E. Amitay-Sadovsky, U. Banin, *J. Am. Chem. Soc.* **2006**, *128*, 10006 – 10007; d) A. Figuerola, I. R. Franchini, A. Fiore, R. Mastria, A. Falqui, G. Bertoni, S. Bals, G. V. Tendeloo, S. Kudera, R. Cingolani, L. Manna, *Adv. Mater.* **2009**, *21*, 550 – 554.

[2] a) V. Subramanian, E. E. Wolf, P. V. Kamat, *J. Am. Chem. Soc.* **2004**, *126*, 4943 – 4950; b) R. Costi, A. E. Saunders, E. Elmalem, A. Salant, U. Banin, *Nano Lett.* **2008**, *8*, 637 – 641.

[3] J. Yang, H. I. Elim, Q. Zhang, J. Y. Lee, W. Ji, *J. Am. Chem. Soc.* **2006**, *128*, 11921 – 11926.

[4] a) M. Casavola, V. Grillo, E. Carlino, C. Giannini, F. Gozzo, E. F. Pinel, M. A. Garcia, L. Manna, R. Cingolani, P. D. Cozzolli, *Nano Lett.* **2007**, *7*, 1386 – 1395; b) J. Maynadié, A. Salant, A. Falqui, M. Respaud, E. Shaviv, U. Banin, K. Soulantica, B. Chaudret, *Angew. Chem.* **2009**, *121*, 1846 – 1849; *Angew. Chem. Int. Ed.* **2009**, *48*, 1814 – 1817; c) S. Deka, A. Falqui, G. Bertoni, C. Sangregorio, G. Poneti, G. Morello, M. D. Giorgi, C. Giannini, R. Cingolani, L. Manna, P. D. Cozzoli, *J. Am. Chem. Soc.* **2009**, *131*, 12817 – 12828.

[5] D. V. Talapin, J. H. Nelson, E. V. Shevchenko, S. Aloni, B. Sadtler, A. P. Alivisatos, *Nano Lett.* **2007**, *7*, 2951 – 2959.

[6] G. Dukovic, M. G. Merkle, J. H. Nelson, S. M. Hughes, A. P. Alivisatos, *Adv. Mater.* **2008**, *20*, 4306 – 4311.

[7] a) G. Menagen, D. Mocatta, A. Salant, I. Popov, D. Dorfs, U. Banin, *Chem. Mater.* **2008**, *20*, 6900 – 6902; b) L. Carbone, A. Jakab, Y. Khalavka, C. Sönnichsen, *Nano Lett.* **2009**, *9*, 3710 – 3714.

[8] a) G. Menagen, J. E. Macdonald, Y. Shemesh, I. Popov, U. Banin, *J. Am. Chem. Soc.* **2009**, *131*, 17406 – 17411; b) D. V. Talapin, R. Koeppe, S. Götzinger, A. Kornowski, J. M. Lupton, A. L. Rogach, O. Benson, J. Feldmann, H. Weller, *Nano Lett.* **2003**, *3*, 1677 – 1681; c) S. E. Habas, P. Yang, T. Mokari, *J. Am. Chem. Soc.* **2008**, *130*, 3294 – 3295.

[9] J. Yang, H. I. Elim, Q. Zhang, J. Y. Lee, W. Ji, *J. Am. Chem. Soc.* **2006**, *128*, 11921 – 11926.

[10] P. T. Snee, Y. Chan, D. G. Nocera, M. G. Bawendi, *Adv. Mater.* **2005**, *17*, 1131 – 1136.

[11] L. Carbone, C. Nobile, M. D. Giorgi, F. B. Sala, G. Morello, P. Pompa, M. Hytch, E. Snoeck, A. Fiore, I. R. Franchini, M. Nadasan, A. F. Silvestre, L. Chiodo, S. Kudera, R. Cingolani, R. Krahne, L. Manna, *Nano Lett.* **2007**, *7*, 2942 – 2950.

[12] A. E. Saunders, I. Popov, U. Banin, *J. Phys. Chem. B* **2006**, *110*, 25421 – 25429.

[13] a) Z. A. Peng, X. Peng, *J. Am. Chem. Soc.* **2001**, *123*, 1389 – 1395; b) S. Kudera, L. Carbone, M. F. Casula, R. Cingolani, A. Falqui, E. Snoeck, W. J. Parak, L. Manna, *Nano Lett.* **2005**, *5*, 445 – 449.

[14] R. D. Robinson, B. Sadtler, D. O. Demchenko, C. K. Erdonmez, L. W. Wang, A. P. Alivisatos, *Science* **2007**, *317*, 355 – 358.

[15] D. R. Lide, *CRC Handbook of Chemistry and Physics*, CRC, Boca Raton, FL, **2000**, pp. 9 – 52.

